

Influence of the splicing on the birefringence characteristics of the highly birefringent photonic crystal fiber

Su Juan¹, Xiaopeng Dong^{1*}, Gan-bin Lin¹, Hao Jiajian¹, Zhidong Shi²

1. Institute of Lightwave Technology, School of Information Science and Technology

Xiamen University, Xiamen, China

2. Key Laboratory of Specialty Fiber Optics and Optical Access Networks, Shanghai University, 200072 Shanghai

ABSTRACT

Influence of splicing the highly birefringent photonic crystal fiber (HB-PCF) with single mode fiber (SMF) under two different experimental conditions is studied in details. The result shows the birefringence of the HB-PCF can be either increased or decreased significantly, depending on the connection conditions of the HB-PCF end, which are classified as case I (the end is closely butted by another fiber) and case II (the end is in open air). From the experiment and theoretical analysis, it has shown that in case I the retardation change of the spliced section of HB-PCF with 0.2mm in length can be 3.2 times larger than the original value. However, in case II the retardation may be reduced to 72.12% of the original one. The obtained result is important for the design and fabrication of optical fiber devices and sensors based on HB-PCFs.

Keywords : photonic crystal fiber; birefringence; splicing;

1. INTRODUCTION

Photonic Crystal Fibers (PCFs) provide great potential and possibilities for the design and development of various devices and components applicable in the areas of optical fiber communications, optical fiber sensors^{[1][2]}, etc. In practical application, connecting PCFs with other types conventional fiber, in most case with the SMFs, is necessary and unavoidable. Since the structures of the cross section of PCF and SMF are distinctly different, how to splice PCF with low insertion loss become a non-ignorable technique in the application of PCF. Several methods have been proposed to reduce the splicing loss including: designing special PCFs that have the same modal field diameters as SMFs^[4]; using a gradient-index fiber lens^{[5][6]} and CO₂ lasers to splice^{[7][8]}; using fusion splicers by repeated discharging to cause collapse of the air holes^{[9][10]}, etc. Since it is easy to implement with splicer, the last method has been widely adopted in practice.

The PCF with two large air holes symmetrically located beside the core may have introduced large birefringence in the fiber. The birefringence strongly depends on the sizes and separations of the air holes. In the condition of fiber splicing, since the arc may produce sufficient high temperature which will cause significant change in the size of the air holes, it is reasonable to expect the birefringence of HB-PCF will change after it has been spliced. As most researchers focus on the loss problem in the splicing of PCF, to our knowledge we studied at the first time the effect of splicing on the birefringence of HB-PCF. We divided the splicing conditions into two cases, i.e. (1) splicing the PCF with closed end (case I); and (2) splicing the PCF with open end (case II). Since the size changes of the air hole are completely different in these two cases, we study the birefringence change of the HB-PCF separately, and analyze the influence of non-uniform birefringence change on the characteristics of fiber waveplate proposed by the authors. The experimental and theoretical results are useful for the development of fiber devices and sensors based on HB-PCFs.

2. EXPERIMENT RESULTS OF DIFFERENT SPLICING CONDITIONS

The HB-PCF used in this article is obtained previously from the Blaze Photonic Company, which is shown in Fig. 1(a). It can be seen from Fig. 1(a) that this kind of HB-PCF is realized by breaking the symmetry of the hexagonal lattice. The fiber parameters including the diameters (d_s) of two large airholes, the diameters (d) of small airholes, the pitch between the two big airholes (Λ_s) and the lattice pitch between the small airholes (Λ) are measured through the optical microscope: $d_s=4.58\mu\text{m}$, $d=2.34\mu\text{m}$, $\Lambda=4.18\mu\text{m}$, $\Lambda_s=8.70\mu\text{m}$. Based on the structure, the air-holes expansion or collapse effect on the birefringence of HB-PCF is calculated by the software APSS of the Appolo Photonics company in Canada, which is based on the full vector finite-difference time-domain (FDTD) method.

*Correspondence author, Email: xpd@xmu.edu.cn

In the experiment, an optical fusion splicer produced by DVP Optical&Electronical Tech Company in Nanjing, China, was employed to splice the HB-PCF with SMF. Under the manual operate condition; we change fusion intensity to 40 and fusion time to 0.5s. Considering the HB-PCFs and PCFs need different melting temperature, appropriate offset should be set as fig.2 (a) ^[13]. When discharging, there is a discharged area. The temperature will transit along the HB-PCF in the discharged area, so there is a expand part or collapse part after splicing. We realized splicing in case I shown in Fig.2 (b) and splicing in case II shown in Fig.2(c) differently by repeated experiment. The airholes of the cross section of the interface expand as shown in Fig.1. (b) , but the airholes of airholes of the cross section of the interface after splicing in case II collapse as shown in Fig.1 (c).

We can observe from Fig.1 (b) that the cross section of the splicing interface changes a lot: the two large holes changes to be approximate hexagon and the small hole expand. After repeated measurements, we got the components: $ds'=5.94\mu\text{m}$, $d_1'=2.72\mu\text{m}$, $\Lambda'=4.26\mu\text{m}$, $\Lambda_s'=7.72\mu\text{m}$. When splicing in case I, high energy gathered in the interface of the HB-PCF which is close with the interface of SMF, though pressure difference in and out the airholes which is much very probably larger than surface tension will cause airholes expand. The large airholes were pressed from six directions, so the large airholes are approximate hexagon. For the air-silica alternating structure, heat flow in the air is slower than the heat flow in the silica^[7], which cause the airholes far away from the core are larger than that near the core, but since they are far away from the core, the effect can be ignored.

We can observe from Fig.1 (c) that the cross section of the splicing interface changes a lot too: both large and small airholes collapse in different degrees. That is because splicing in case II, the pressure in and out the airholes is equal and the surface tension is much larger than the pressure ^[12]. By repeated measurements, we got the components: $ds''=2.90\mu\text{m}$, $d_1''=1.9\mu\text{m}$, $\Lambda''=6.58\mu\text{m}$, $\Lambda_s''=6.60\mu\text{m}$.

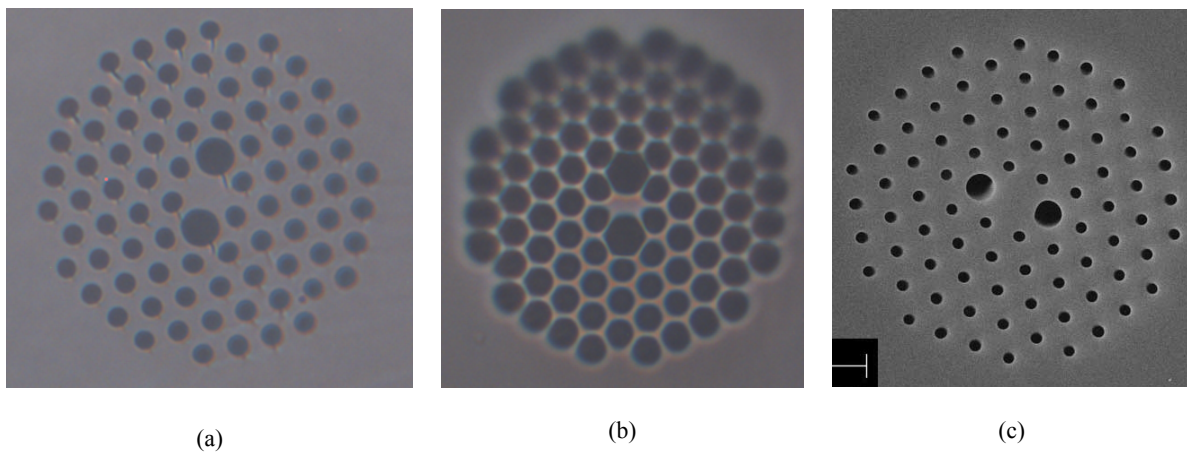
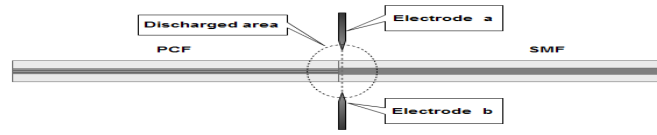


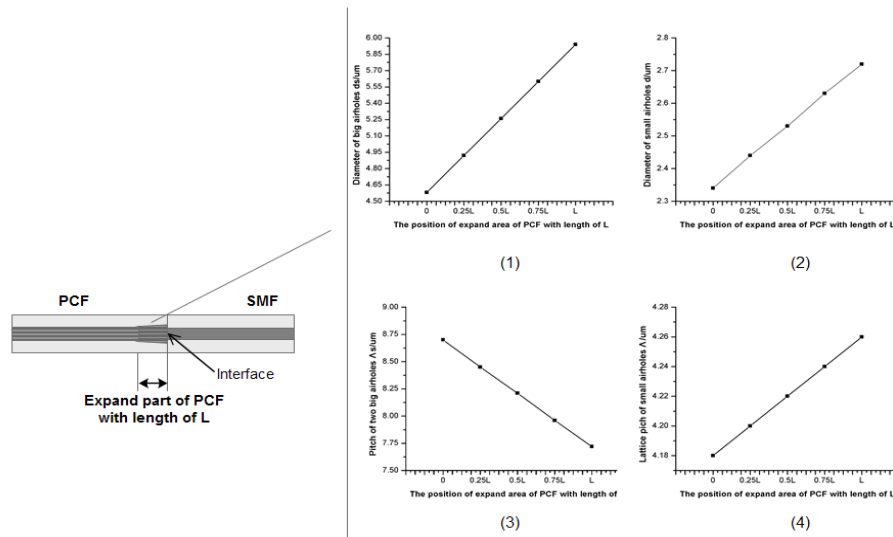
Figure 1. Optical microscope images of HB-PCF cross section before and after splicing . (a)Optical microscope image of HB-PCF before splicing ; (b)Optical microscope image of HB-PCF after splicing in case I with expanded airholes ; (c)SEM image of HB-PCF after splicing in case II with collapse airholes^[9]

3. THE SIMULATED RESULT OF EFFECT ON THE BIREFRINGENCE OF THE CROSS SECTION OF HB-PCF AFTER SPLICING

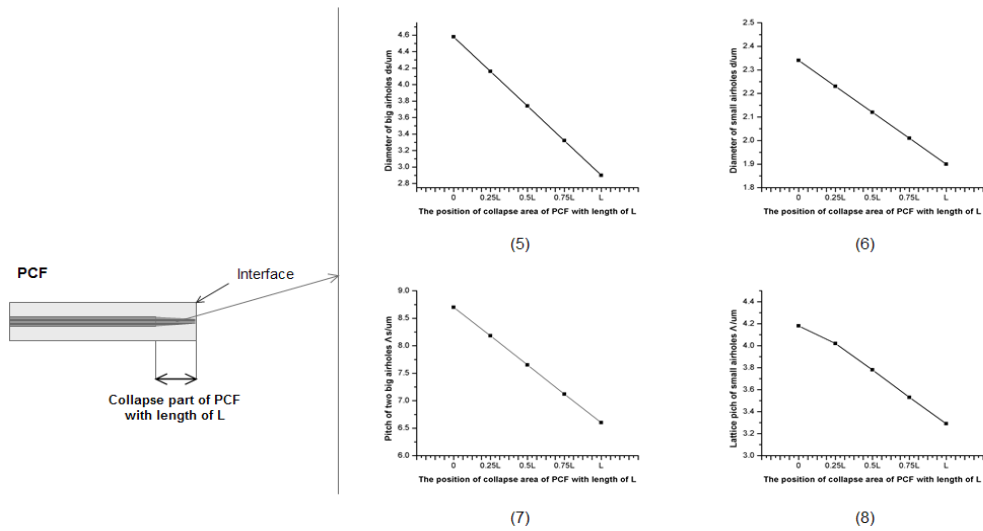
The model birefringence of the interface cross sections after spliced in case I and case II is simulated numerically. The result is shown in Fig.3. We know that after splicing in case I, ds increased 29.69%, d increased 16.24%, Λ_s decreased 11.26% and Λ increased 8%, they all affect the birefringence a lot. We can observe from Fig.3 that the birefringence is 5.6 ~ 5.8 times larger than that before splicing. And the birefringence changing as a function of the wavelength becomes much sensitive. But in condition of case II, ds decreased 36.68%, d decreased 18.8%, Λ_s decreased 24.14% and Λ decreased 21.29%. The birefringence decreased $6 \times 10^{-5} \sim 8 \times 10^{-5}$. We can conclude that the airholes expansion and collapse will change the birefringence of HB-PCF differently. So during the use for the birefringence character of HB-PCF, especially for the waveplate fabricated by HB-PCF, splicing effect on the length or band of the waveplate must be considered.



(a)



(b)



(c)

Figure 2. General view of splicing PCF and SMF in case I and side view of HB-PCF after splicing (a) General view of splicing PCF and SMF in case I ; (b) The side view of the interface of HB-PCF and SMF spliced in case I ((1)(2)(3)(4)are the supposed size of the parameters d_s 、 d 、 Λ_s and Λ in the expand part of PCF) ; (c)The side view of the interface of HB-PCF after discharged in case II ((5)(6)(7)(8)are the supposed size of the parameters d_s 、 d 、 Λ_s and Λ in the collapse part of PCF)

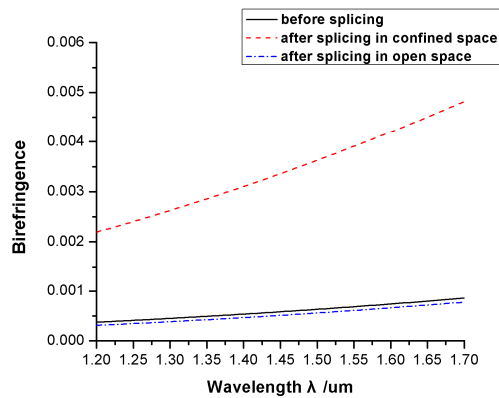


Figure 3. The birefringence as a function of wavelength before splicing and after splicing in different splicing method

3. THE SIMULATED RESULT OF EFFECT ON THE BIREFRINGENCE OF THE EXPAND OR COLLAPSE PART OF HB-PCF AFTER SPLICING

Supposing that the hot flow along the PCF is linearly, the airholes of the expand part shown in Fig.2 (b) or the collapse part shown in Fig.2 (c) change linearly, as shown (1) ~ (8) in Fig.2(b) and (c). Based on this, we founded numerical calculation model and simulated the birefringence as a function of the position of the expand part or the collapse part, which is shown in Fig.4.

Fig.4 (a) shows the fitted curve about birefringence as a function of the position of the expand part at the wavelength of 1550nm. Due to the accuracy of the calculation method, the spots are not on the line. It is observed from Fig. (4) that the birefringence of HB-PCF increase in form of exponential growth during the expand part. And the birefringence can up to 5.8 times larger than usual. Because both the large and small holes expanded, Δs decreased and Λ increased, all of this destroyed the symmetrical hexagon structure. And it is why the birefringence becomes much larger when the cross sections near the interface of splicing. Fig. 4 (b) shows the curve about birefringence as a function of the position of the collapse part at the wavelength of 1550nm. Obviously it is different from Fig.4 (a). After spliced incase II, the birefringence decreases with rule during the collapse part. This is caused by two reasons: one is that the sizes of both the large and small airholes decreased, while the large airholes change more than the small ones. This cause model birefringence reducing shown in Fig.5 (a); the other one is that Δs and Λ both decreased, which destroyed the symmetrical hexagon structure and caused the model birefringence decrease shown in Fig.5 (b). The result shown in Fig.4 (b) is caused by these two reasons interacting by some ways.

Fig.5 (a) shows the model birefringence as a function of the collapse part, supposing that only the size of airholes was changed during the collapse part of the HB-PCF. The model birefringence's reduction caused by the size reduction of the large and small airholes is proved. Fig. 5(b) shows the model birefringence as a function of the collapse part, supposing that only the distances of large airholes or small airholes was changed during the collapse part of the HB-PCF. The model birefringence increase by reason of the damage of the symmetrical hexagon structure is proved.

The relationship of the phase difference δ and the model birefringence B of two orthogonal models is given by

$$B = n_y - n_x = \frac{\beta_y - \beta_x}{k_0} = \frac{\Delta\beta}{k_0}, (k_0 = \frac{2\pi}{\lambda}) \quad (1)$$

$$\delta = \Delta\beta \times l = B \times k_0 \times l \quad (2)$$

n_y , n_x , β_y and β_x are effective index and propagation constant of two orthogonal models, λ is the wavelength and l is the length of optical fiber. If the wavelength is fixed, and B is the function of l , we make it $B(l)$, an integral function is used to calculate δ :

$$\delta = \int_0^L B(l)dl \quad (3)$$

Proved by repeated experiment and calculation, the length of the expand part or collapse part is 0.15mm ~ 0.2mm. When the wavelength is fixed at 1550nm, supposing the expand part or collapse part is 0.22mm long, the phase difference $\delta=0.556\text{rad}$ before splicing, according to equation (2). But the phase difference turns to be $\delta=1.802\text{rad}$ after splicing in case I, according to equation (3), which is 3.2 times larger than that before splicing. The phase difference turns to be $\delta=0.401\text{rad}$ after splicing in case II, according to equation (3), which is 27.88% of that before splicing. We can observe the conclusion: both the airholes expansion and collapse will cause δ change a lot. This is very important for fiber waveplate fabricated by PCFs.

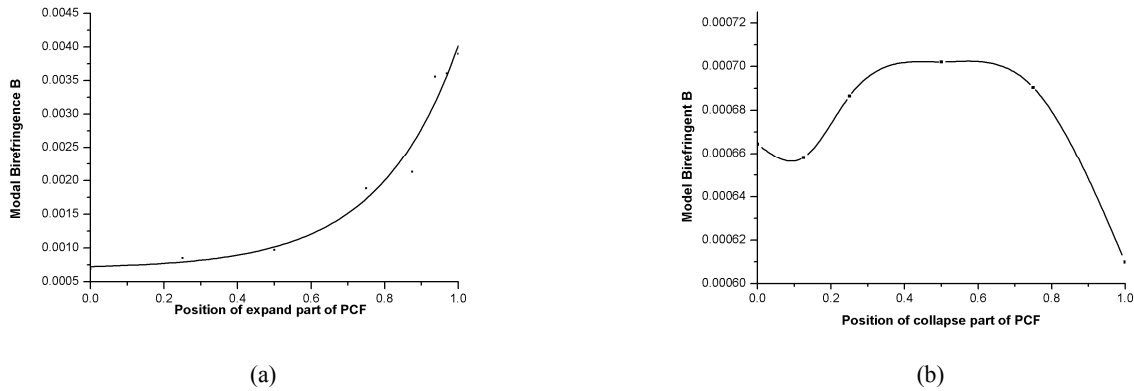


Figure 4. The model birefringence as a function of expand or collapse part of PCF under different splicing condition @ $\lambda=1550\text{nm}$ ((a) The model birefringence of the expand part of PCF after spliced in case I ; (b) The model birefringence of the collapse part of PCF after discharged in case II)

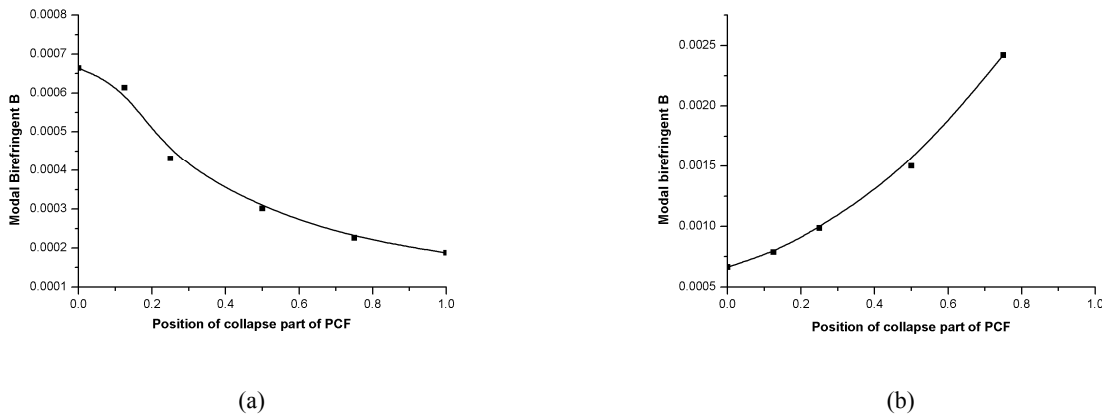


Figure 5. The model birefringence as a function of the collapse part of PCF after discharged in case II, supposing only sizes of airholes or pitch between holes changed . ((a) When the size of airholes change as (5)(6)in Fig . 3(b) only ; (b) When the pitch between holes change as (7)(8) in Fig . 3(b)only)

ACKNOWLEDGMENT

This work is supported by the National Science Foundation of China under the Grant No. 61077031.

REFERENCES

1. J. C. Knight, T. A. Birks, P. St. J. Russell and D. M. Atkin, "All-silica single-mode optical fiber with Photonic crystal cladding" *Optics Letters*, American, vol. 21, pp. 1547–1549, 1996.
2. Jonathan C. Knight, "Photonic crystal fibres". *Nature*, England, vol. 424, pp. 847–851, 2003.
3. P. J. Bennet, Tanya M. Monro, and D. J. Richardson, "Toward practical holey fiber technology: fabrication, splicing, modeling, and characterization", *Optics Letters*, American, vol. 24, pp. 1203–1205, 1999.
4. Yeuk Lai Hoo, Wei Jin, Jian Ju, and Hoi Lut Ho, "Loss Analyses Of Single-mode Fiber/Photonic-Crystal Fiber Splice", *Microwave and Optical Technology Letters*, vol. 40, pp. 378–380, 2004.
5. A. D. Yablon and R. Bise, "Low-Loss High-Strength Microstructured Fiber Fusion Splices Using GRIN Fiber Lenses", *IEEE Photonics Technology Letters*, vol. 17, pp. 118–120, 2005.
6. Zhang Wei, Zhang Lei, Chen Shi, Cai Qing, et al.. "Low Loss Splicing Experiment of High Nonlinearity Photonic Crystal Fiber and Single Mode Fiber", *Chinese Journal of Laser*, vol. 33, pp. 1389–1392, 2006.
7. Joo Him Chong and M. K. Rao, "Development of a system for laser splicing photonic crystal fiber", *Optics Express*, vol. 11 pp. 1365–1370, 2003
8. Chen Mingguo, Zhao Shanghong, Dong Shufu, et al.. "Study on Splicing Method of Photonic Crystal Fiber", *Optical Communication Technology*, vol. 7 pp. 23–25. 2004.
9. Limin Xiao, M. S. Demokan, Wei Jin, Yiping Wang and Chun-Liu Zhao, "Fusion Splicing Photonic Crystal Fibers and Conventional Single-Mode Fibers: Microhole Collapse Effect", *Journal Of Lightwave Technology*, vol. 25, pp: 3563–3574, 2007.
10. Guo Tiejing, Lou Shuqin, Li Honglei, Yao Lei, Jian Shuisheng,, "Low Loss Arc Fusion Splice of Photonic Crystal Fibers", *Acta Optica Sinica*, vol. 29, pp: 511–516, 2009.
11. Xiaopeng Dong, Xie Zuosheng, Wang Xiaozhen, Jin Hailan. "Design and analysis of novel wave-plate made by the photonic crystal fibers", National Standardization Technical Committee, G02B 6/02 ; G02B 6/38, 2007
12. Fu Guangwei, Bi Weihong, Jin Wa. "Mechanics Characteristic of Air-Hole in Fusion Splicing Process for Photonic Crystal Fiber", *Chinese Journal Of Lasers*, vol. 36 pp: 2966–2970, 2009.
13. James C. Fajardo, Painted Post, Michael T. Gallagher, Qi Wu, Eaton Town. "Splice joint and process for joining a microstructured optical fiber and a conversional fiber", United States Patent Application Publication, G02B 6/255, 2003.